Electronic Supplementary Material (ESI) for Sustainable Energy & Fuels.


# Supporting Information

## Molecular Engineering of Simple Carbazole-Arylamine Hole-Transport Materials for Perovskite Solar Cells

Xuepeng Liu,[1,a] Shuang Ma,[1,a] Muhammad Mateen,[a] Pengju Shi,[a] Cheng Liu,[a,b] Yong Ding,[a,b] Molang Cai,[a] Mina Guli,[a] Mohammad Khaja Nazeeruddin,*[b] Songyuan Dai*[a]

[a] Beijing Key Laboratory of Novel Thin-Film Solar Cells, School of Renewable Energy, North China Electric Power University, Beijing, 102206, P. R. China. E-mail: sydai@ncepu.edu.cn

[b] Group for Molecular Engineering of Functional Materials Institute of Chemical Sciences and Engineering, École Polytechnique Fédérale de Lausanne (EPFL) CH-1951 Sion, Switzerland. E-mail: mdkhaja.nazeeruddin@epfl.ch

**Table S1** The average photovoltaic parameters of n-i-p $(FAPbI_3)_{0.85}(MAPbBr_3)_{0.15}$-based PSCs with different additive-free HTMs.

| HTM | Concentration (mg mL$^{-1}$) | $V_{oc}$ (V) | $J_{sc}$ (mA cm$^{-2}$) | FF (%) | PCE (%) |
|---|---|---|---|---|---|
| **3,6-O** | 10 | 1.01 ± 0.02 | 17.12 ± 0.73 | 58 ± 1.94 | 10.10 ± 0.59 |
| **3,6-O** | 20 | 1.05 ± 0.01 | 19.20 ± 0.37 | 65 ± 1.07 | 13.23 ± 0.45 |
| **3,6-O** | 30 | 1.03 ± 0.01 | 18.69 ± 0.32 | 64 ± 0.87 | 12.43 ± 0.18 |
| **3,6-O** | 45 | 1.03 ± 0.01 | 18.21 ± 0.39 | 61 ± 0.79 | 11.49 ± 0.10 |
| **3,6-N** | 10 | 1.01 ± 0.02 | 18.71 ± 0.39 | 65 ± 0.87 | 12.48 ± 0.36 |
| **3,6-N** | 20 | 1.04 ± 0.01 | 20.09 ± 0.57 | 73 ± 1.87 | 15.28 ± 0.72 |
| **3,6-N** | 30 | 1.01 ± 0.02 | 16.82 ± 0.42 | 59 ± 0.79 | 10.06 ± 0.48 |
| **3,6-N** | 45 | 0.91 ± 0.03 | 15.24 ± 0.56 | 49 ± 1.62 | 6.82 ± 0.39 |
| **3,6-S** | 10 | 1.01 ± 0.02 | 17.75 ± 0.29 | 50 ± 1.90 | 10.70 ± 0.35 |
| **3,6-S** | 20 | 1.04 ± 0.01 | 20.14 ± 0.37 | 70 ± 0.89 | 14.73 ± 0.30 |
| **3,6-S** | 30 | 1.04 ± 0.01 | 19.67 ± 0.25 | 67 ± 0.62 | 13.74 ± 0.39 |
| **3,6-S** | 45 | 1.03 ± 0.01 | 18.91 ± 0.26 | 62 ± 0.77 | 12.11 ± 0.15 |
| **Spiro-OMeTAD** | 20 | 1.01 ± 001 | 19.95 ± 0.24 | 61 ± 0.68 | 012.68 ± 0.24 |

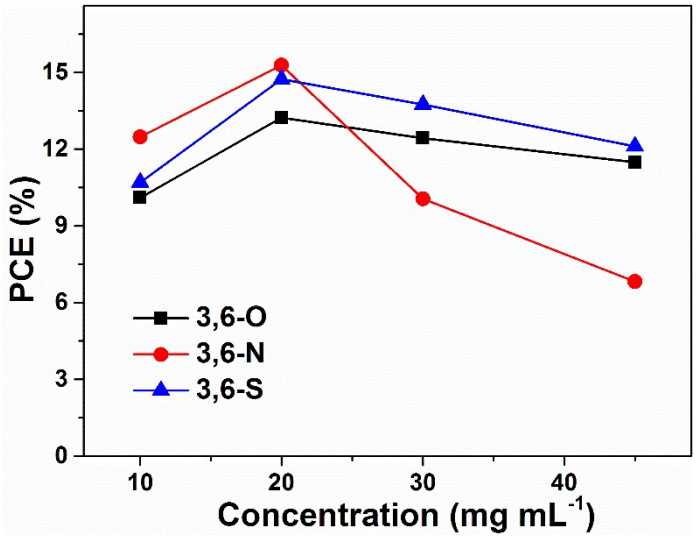


**Fig. S1** The average PCE variations with the concentration change of additive-free **3,6-O**, **3,6-N** and **3,6-S** for Table 1.

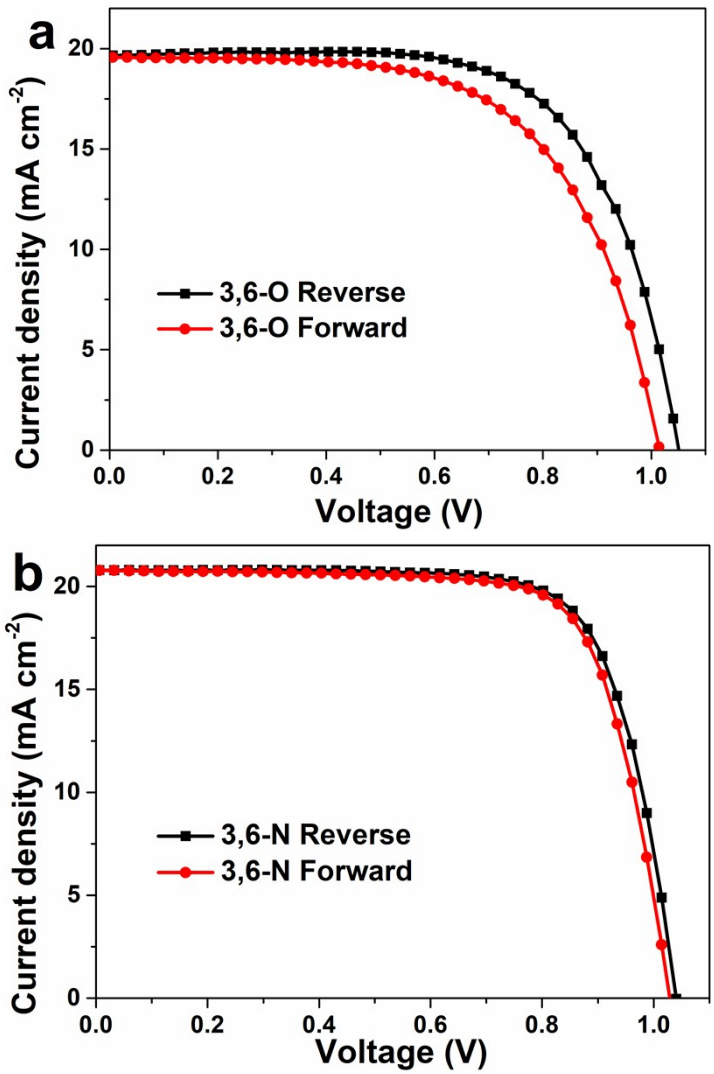

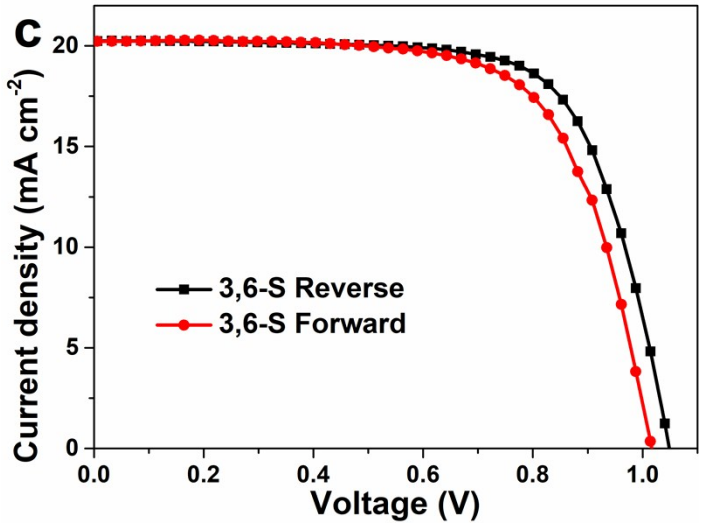


**Fig. S2** *J-V* curves measured by forward scan (from short circuit to open circuit) and reverse scan (from open circuit to short circuit) of the n-i-p $(FAPbI_3)_{0.85}(MAPbBr_3)_{0.15}$-based PSCs with different additive-free HTMs under AM 1.5 illumination.

**Table S2** Photovoltaic parameters of best-performing n-i-p $(FAPbI_3)_{0.85}(MAPbBr_3)_{0.15}$-based PSCs with different additive-free HTMs and measured through forward and reverse scans for Fig. S2.

| HTM | | $V_{oc}$ (V) | $J_{sc}$ (mA cm$^{-2}$) | FF (%) | PCE (%) |
|---|---|---|---|---|---|
| **3,6-O** | Reverse | 1.05 | 19.71 | 67 | 13.84 |
| | Forward | 1.01 | 19.56 | 62 | 12.30 |
| **3,6-N** | Reverse | 1.04 | 20.80 | 74 | 16.12 |
| | Forward | 1.03 | 20.78 | 74 | 15.85 |
| **3,6-S** | Reverse | 1.05 | 20.24 | 71 | 15.01 |
| | Forward | 1.02 | 20.23 | 68 | 14.02 |

**Table S3** The average photovoltaic parameters of n-i-p $(FAPbI_3)_{0.85}(MAPbBr_3)_{0.15}$-based PSCs with different doped HTMs (20 mg mL$^{-1}$).

| **HTM** | **$V_{oc}$ (V)** | **$J_{sc}$ (mA cm$^{-2}$)** | **FF (%)** | **PCE (%)** |
|---|---|---|---|---|
| **3,6-O** | 1.07 ± 0.02 | 21.87 ± 0.53 | 73 ± 1.13 | 17.04 ± 0.26 |

| | | | | |
|---|---|---|---|---|
| **3,6-N** | 1.07 ± 0.01 | 22.06 ± 0.47 | 77 ± 1.85 | 18.21 ± 0.18 |
| **3,6-S** | 1.08 ± 0.01 | 22.04 ± 0.51 | 73 ± 0.98 | 17.37 ± 0.33 |

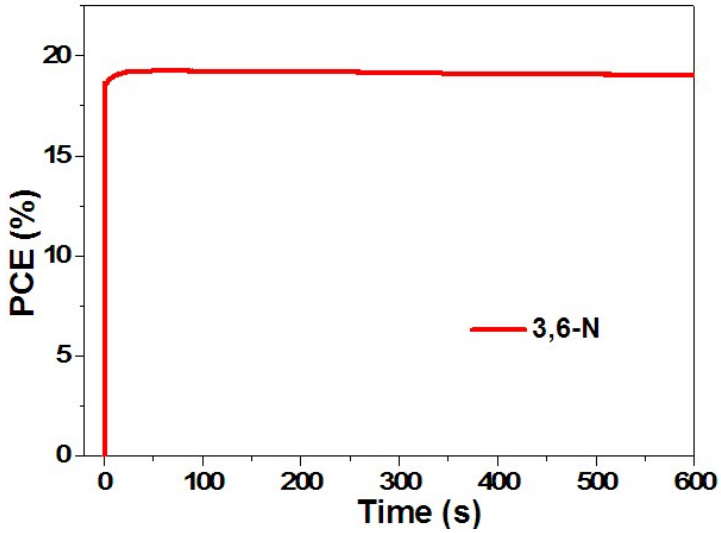


**Fig. S3** The stabilized power output of the best-performing devices with doped 3,6-N, measured at 0.90 V.

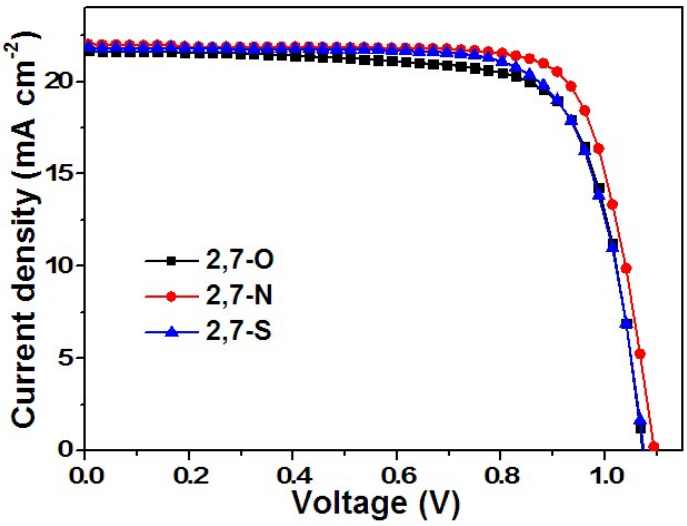


**Fig. S4** *J-V* curves of best-performing n-i-p $(FAPbI_3)_{0.85}(MAPbBr_3)_{0.15}$-based PSCs with doped 2,7-HTMs.

**Table S4** Photovoltaic parameters of the n-i-p $(FAPbI_3)_{0.85}(MAPbBr_3)_{0.15}$-based PSCs with doped 2,7-HTMs for Fig. S4.

| HTM | $V_{oc}$ (V) | $J_{sc}$ (mA cm$^{-2}$) | FF (%) | PCE (%) | PCE$_{avg}$[a] |
|---|---|---|---|---|---|

| | | | | | (%) |
|---|---|---|---|---|---|
| **2,7-O** | 1.07 | 21.67 | 74 | **17.27** | 15.84 |
| **2,7-N** | 1.09 | 22.01 | 77 | **18.65** | 16.17 |
| **2,7-S** | 1.07 | 21.85 | 74 | **17.48** | 15.92 |

[a] Average PCE from 5 independent cells.

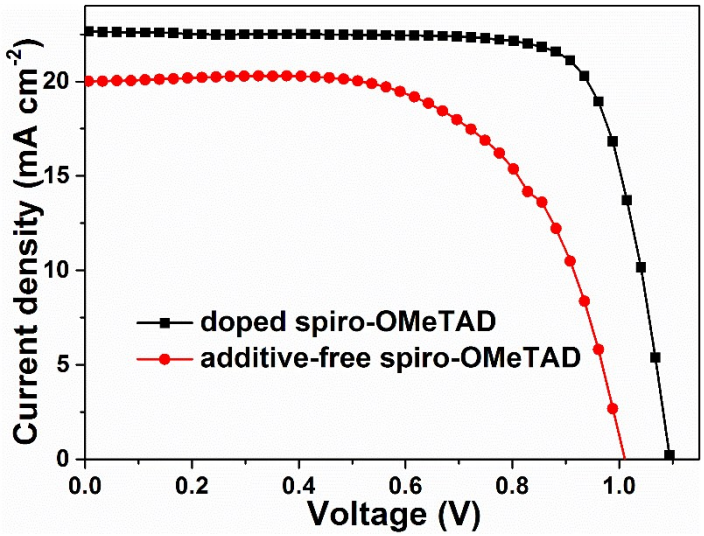


**Fig. S5** *J-V* curves of the best-performing n-i-p $(FAPbI_3)_{0.85}(MAPbBr_3)_{0.15}$-based devices with spiro-OMeTAD, (a) without (20 mg $mL^{-1}$), and (b) with Li-TFSI and TBP (73 mg $mL^{-1}$).

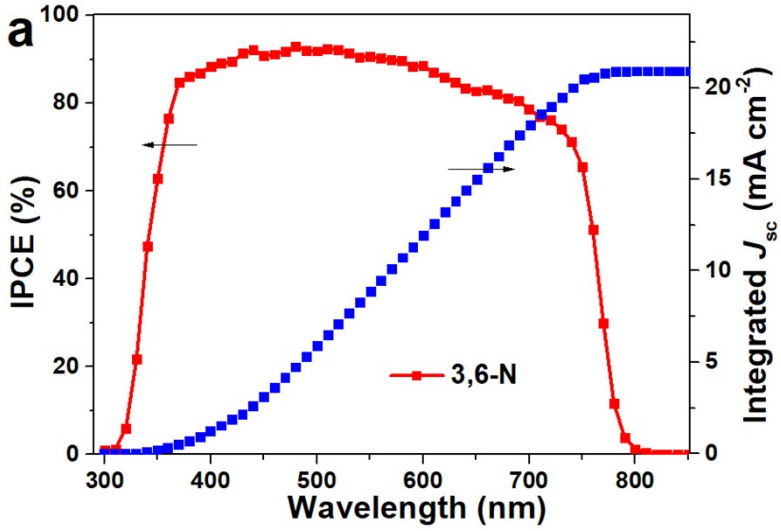

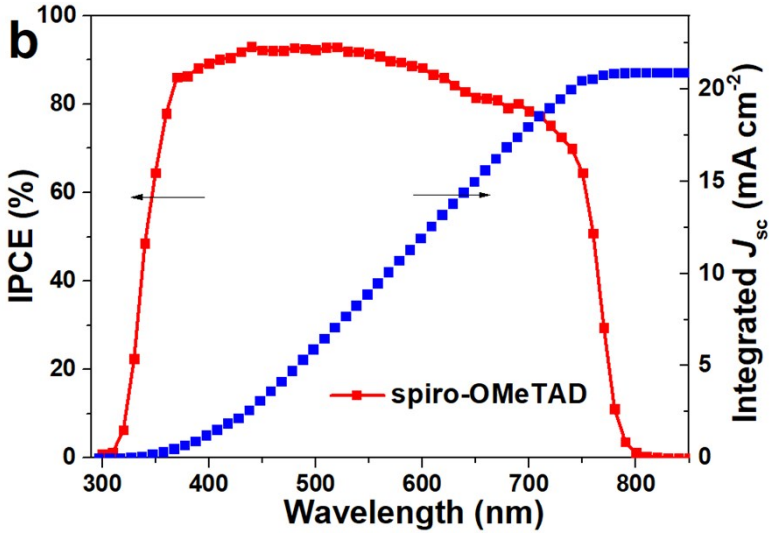


**Fig. S6** (a) The incident photon-to-current conversion efficiency (IPCE) integrated *J*sc spectra of n-i-p $(FAPbI_3)_{0.85}(MAPbBr_3)_{0.15}$-based PSCs with doped **3,6-N** and spiro-OMeTAD.

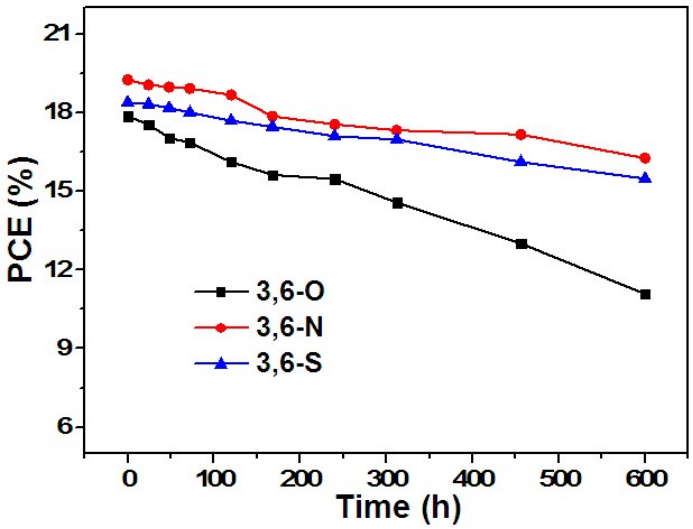


**Fig. S7** The stability of the $(FAPbI_3)_{0.85}(MAPbBr_3)_{0.15}$-based devices employing different HTMs without encapsulation under dark and dry condition.

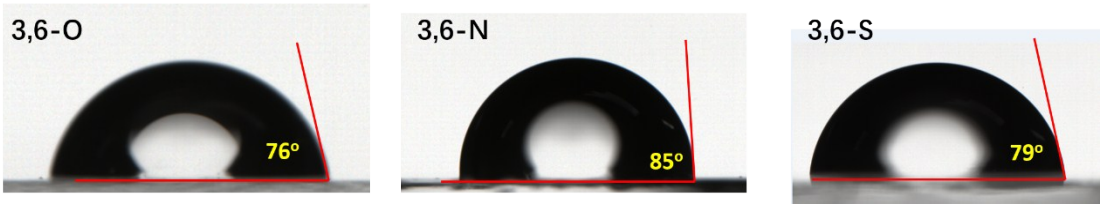


**Fig. S8** Water contact angles of **3,6-O**, **3,6-N** and **3,6-O**.

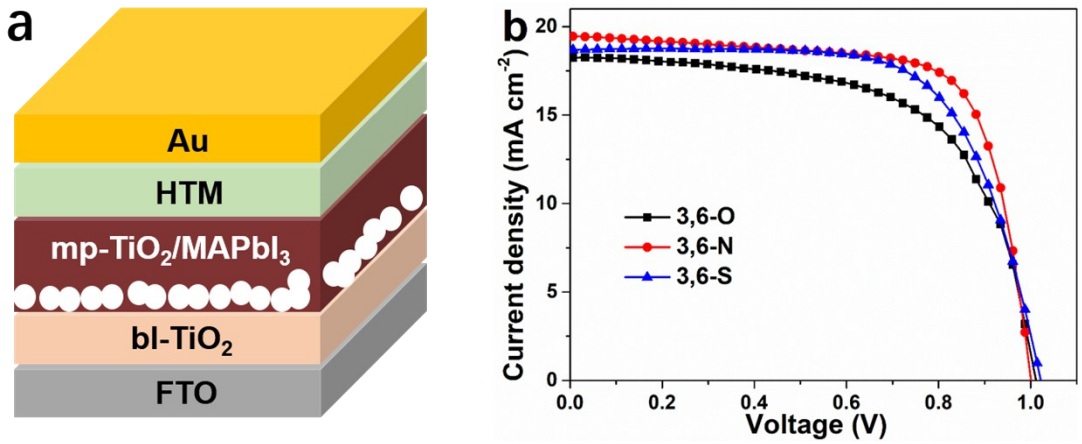


**Fig. S9** The structure of n-i-p $MAPbI_3$-based PSC in this work and corresponding *J-V* curves of best-performing devices employing additive-free HTMs.

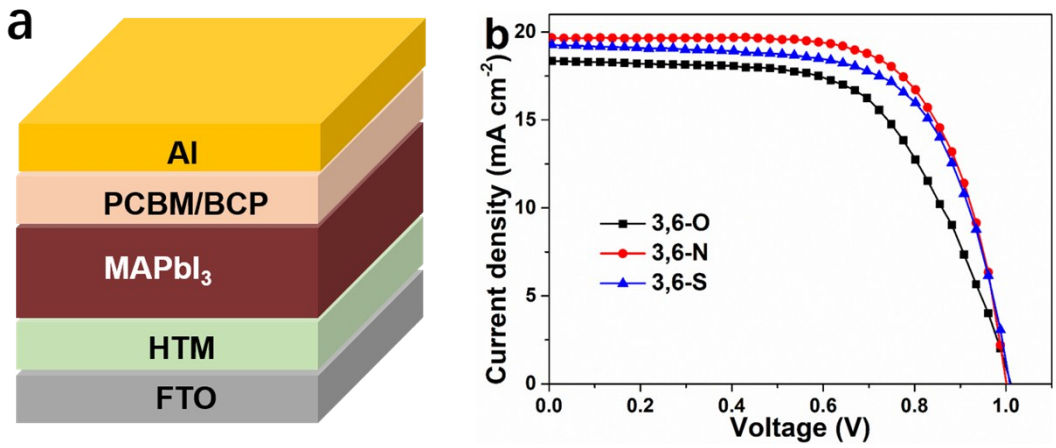


**Fig. S10** The structure of p-i-n $MAPbI_3$-based PSC in this work and corresponding *J-V* curves of best-performing devices employing additive-free HTMs.

**Table S5** Photovoltaic parameters of best-performing n-i-p and p-i-n $MAPbI_3$-based PSCs with pristine HTMs. n-i-p devices: HTM 20 mg $mL^{-1}$; p-i-n devices: HTM 5 mg $mL^{-1}$.

| Device structure | HTM | $V_{oc}$ (V) | $J_{sc}$ (mA $cm^{-2}$) | FF (%) | PCE (%) |
|---|---|---|---|---|---|
| **n-i-p** | **3,6-O** | 1.01 | 18.25 | 62.42 | 11.53 |

| | | | | | |
|---|---|---|---|---|---|
| | **3,6-N** | 1.00 | 19.47 | 72.18 | 14.05 |
| | **3,6-S** | 1.02 | 18.54 | 67.59 | 12.81 |
| **p-i-n** | **3,6-O** | 1.01 | 18.36 | 60.84 | 11.29 |
| | **3,6-N** | 1.00 | 19.52 | 70.14 | 13.72 |
| | **3,6-S** | 1.01 | 19.26 | 66.33 | 12.89 |

**Table S6** The average photovoltaic parameters of n-i-p $MAPbI_3$-based PSCs with different HTMs (without Li-TFSI and TBP).

| **HTM** | **Concentration (mg mL$^{-1}$)** | **$V_{oc}$ (V)** | **$J_{sc}$ (mA cm$^{-2}$)** | **FF (%)** | **PCE (%)** |
|---|---|---|---|---|---|
| **3,6-O** | 10 | 1.00 ± 0.01 | 17.26 ± 0.76 | 60.14 ± 0.84 | 10.35 ± 0.44 |
| **3,6-O** | 20 | 1.01 ± 0.01 | 18.08 ± 0.14 | 63.10 ± 0.95 | 11.53 ± 0.22 |
| **3,6-O** | 30 | 1.00 ± 0.01 | 17.87 ± 0.39 | 61.15 ± 0.25 | 10.93 ± 0.18 |
| **3,6-N** | 10 | 0.96 ± 0.01 | 17.82 ± 0.66 | 66.20 ± 2.54 | 11.28 ± 0.39 |
| **3,6-N** | 20 | 0.98 ± 0.01 | 19.06 ± 0.63 | 70.95 ± 1.03 | 13.29 ± 0.69 |
| **3,6-N** | 30 | 0.90 ± 0.02 | 16.87 ± 0.52 | 54.79 ± 0.69 | 8.27 ± 0.10 |
| **3,6-S** | 10 | 1.01 ± 0.01 | 17.46 ± 0.44 | 62.89 ± 0.70 | 11.12 ± 0.37 |
| **3,6-S** | 20 | 1.02 ± 0.01 | 18.31 ± 0.26 | 66.64 ± 0.94 | 12.45 ± 0.28 |
| **3,6-S** | 30 | 1.01 ± 0.01 | 17.30 ± 0.22 | 64.29 ± 0.56 | 11.24 ± 0.28 |

**Table S7** The average photovoltaic parameters of p-i-n $MAPbI_3$-based PSCs with different HTMs (without Li-TFSI and TBP).

| **HTM** | **Concentration (mg mL$^{-1}$)** | **$V_{oc}$ (V)** | **$J_{sc}$ (mA cm$^{-2}$)** | **FF (%)** | **PCE (%)** |
|---|---|---|---|---|---|
| **3,6-O** | 5 | 1.00 ± 0.02 | 18.14 ± 0.38 | 60.28 ± 1.16 | 10.96 ± 0.33 |

| | | | | | |
|---|---|---|---|---|---|
| **3,6-O** | 10 | 0.95 ± 0.01 | 16.60 ± 0.47 | 54.87 ± 0.51 | 8.61 ± 0.16 |
| **3,6-N** | 5 | 0.98 ± 0.02 | 19.07 ± 0.32 | 69.77 ± 1.15 | 13.05 ± 0.55 |
| **3,6-N** | 10 | 0.91 ± 0.02 | 15.74 ± 0.35 | 65.80 ± 0.64 | 9.43 ± 0.13 |
| **3,6-S** | 5 | 1.02 ± 0.02 | 18.78 ± 0.33 | 65.72 ± 0.44 | 12.59 ± 0.22 |
| **3,6-S** | 10 | 0.96 ± 0.01 | 17.49 ± 0.22 | 60.56 ± 0.71 | 10.16 ± 0.21 |

**Device fabrication**

**n-i-p $MAPbI_3$-based PSCs:** FTO glass plates were sequentially cleaned by ultrasonic bath, water and ethanol. The compact $TiO_2$ layer was deposited on the etched substrate by spray pyrolysis at 450 °C using a precursor solution of 0.6 mL titanium diisopropoxide and 0.4 mL bis(acetylacetonate) in 7 mL anhydrous isopropanol. Mesoporous $TiO_2$ film was deposited on the substrate by spin-coating of a diluted particle $TiO_2$ paste (Dyesol 30NR-T, 1:5 w/w diluted in ethanol) at 5500 rpm for 20 s. Then the substrates were sintered at 510 °C for 30 min. After cooling down, the perovskite layer was deposited by spin-coating the perovskite precursor solution by a single step procedure. The perovskite precursor solution contained $PbI_2$ (1.15 M) and MAI (1.1 M), dissolved in a mixed solvent of DMF and DMSO solution (800 µL, volume ratio 1:4). The spin-coating procedure was carried out first 2000 rpm for 10 s, second 5000 rpm for 30 s. 90 µL chlorobenzene was poured on the spinning substrate during the second spin-coating step 15 s before the end of the procedure. The substrate was immediately heated at 100 °C for 1h on a hotplate. The HTM was subsequently deposited on the substrate by spin-coating at 3000 rpm for 20 s. The HTM solution (10-30 mg $mL^{-1}$) were prepared in anhydrous toluene, which is used without dopants. Finally, a ~60 nm thick Au counter electrode was deposited on top of the film by thermal evaporation. The active area of the device was defined by a black mask with a size of 0.09 $cm^2$ for all measurement.

**n-i-p $(FAPbI_3)_{0.85}(MAPbBr_3)_{0.15}$-based PSCs:** The mainly fabricated procedures of n-i-p

$(FAPbI_3)_{0.85}(MAPbBr_3)_{0.15}$-based PSCs is same with n-i-p $MAPbI_3$-based ones. The difference are as follows. The perovskite precursor solution contained $PbBr_2$ (0.2 M), MABr (0.2 M), $PbI_2$ (1.13 M) and FAI (1.1 M) dissolved in a mixed solvent of DMF and DMSO solution (800 µl, volume ratio 1:4). The spin-coating procedure was carried out first 2000 rpm for 10 s, second 5000 rpm for 30 s. 90 µl chlorobenzene was poured on the spinning substrate during the second spin-coating step 15 s before the end of the procedure. The substrate was immediately heated at 100 °C for 1.5 h on a hotplate. The HTM deposited procedure of the devices without dopants was same with n-i-p MAPbI3-based PSCs. When the HTM is doped, The HTMs were dissolved in anhydrous toluene (45 mg $mL^{-1}$) with 15 µL of 4-tert-butylpyridine and 8 µL of lithium bis(trifluoromethylsulphonyl)imide (520 mg $mL^{-1}$ in acetonitrile). The solution is diluted with certain proportion to reduce the concentration.

**p-i-n $MAPbI_3$-based PSCs:** The HTMs were prepared on FTO substrates by spin-coating its chlorobenzene (CB) solutions with the concentration of 5 mg $mL^{-1}$ at the speed of 3000 rpm for 30 s, respectively, and then annealed at 100 $^oC$ for 10 min. The stoichiometry perovskite precursor solution (1.2 M, $PbI_2$ and MAI with a molar ratio of 1:0.98 in mixed-solvent of DMF:DMSO=4:1) was deposited onto the prepared HTL films at 1100 rpm for 10 s and 4200 rpm for 30s. 110 µL chlorobenzene was quickly dripped onto the spinning film at 10 s before the end of the procedure. After that, the deposited films were thermal annealed at 100 $^oC$ for 15 min in a nitrogen-filled glove-box. The resulting perovskite films were coated with $PC_{60}BM$ film by spin-coating 20 mg $mL^{-1}$ $PC_{60}BM$ solution (in CB) at 2000 rpm for 30s, followed by spin-coating the bathocuproine (BCP) solution (0.5 mg $mL^{-1}$ in isopropanol) at 6000 rpm for 30 s. Finally, the devices were completed by depositing the Ag electrode. The active area of the device was defined by a black mask with a size of 0.1225 $cm^2$ for all measurement.

**Instrumentation**

$^1H$ NMR spectra were carried out on a Brücker spectrometer (400 MHz) with chemical

shifts against tetramethylsilane (TMS). Time-of-flight mass spectrometer (MALDI-TOF-MS) experiments were recorded using a MS Bruker Daltonik Reflex III and Bruker solariX spectrometer. The steady-state photoluminescence measurements were obtained from a Fluorescence Detector (Fluorolog-3, HORIBA, USA) with a standard 450 W xenon CW lamp. Cyclic voltammetry was recorded on a CHI660d electrochemical analyzer (CH Instruments, Inc., China). A normal three electrode system was used consisting of a platinum working electrode, a platinum wire counter electrode, and a calomel reference electrode. Redox potential of them was measured in DCM with 0.1 M tetrabutylammonium hexafluorophosphate with a scan rate of 50 mV $s^{-1}$ (*vs.* $Fc/Fc^{+}$ as an external reference). The UV-vis spectra were measured on a U3900H UV-Vis spectrophotometer (Hitachi, Japan). The current-voltage (*J*-*V*) characteristics of the PSCs were carried out under AM 1.5G (100 mW $cm^{-2}$) illumination that was provided by a 3A grade solar simulator (Newport, USA, 94043A). The incident photon-to-current conversion efficiency (IPCE) was recorded on QE/IPCE measurement kit (Newport, USA). The morphologies of the samples were investigated by atomic force microscopy (5500 AFM (Agilent Technologies)).

**Materials and Synthesis of HTMs**

All chemicals and reagents were purchased from TCI, Alfa, Sigma-Aldrich or Sinopharm Chemical Reagent Co.. Toluene was dehydrated by 4Å molecular sieves. Other chemicals were used as received with further processing. The final products are synthesized *via* Buchwald-Hartwig and Suzuki-Miyaura cross-coupling reaction, respectively. The detailed synthetic procedures of them are shown as follows.

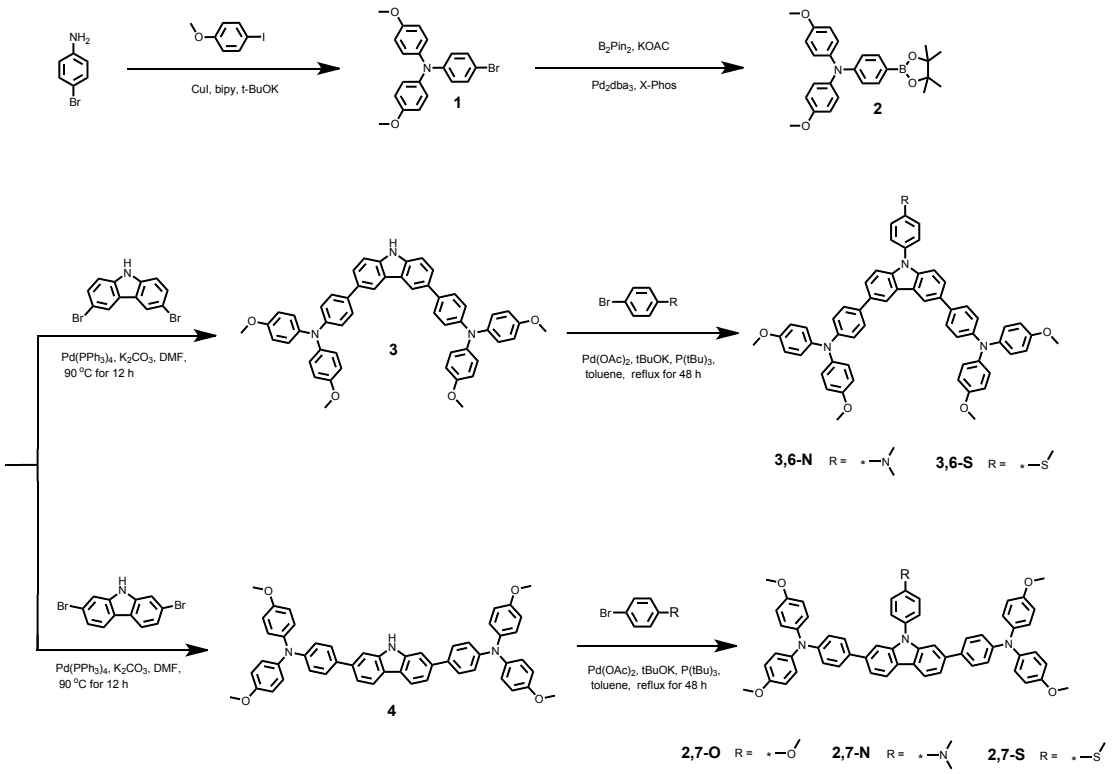


**Scheme S1** Synthetic routes to investigated HTMs in this work. The structures of target HTMs is confirmed by NMR, elemental analysis and HRMS (MALDI-TOF) measurements.

**4-bromo-N,N-bis(4-methoxyphenyl)aniline (compound 1)[1, 2]**

4-Bromoaniline (3.4 g, 20 mmol), 4-iodoanisole (20 g, 80 mmol), CuI (0.15 g, 0.85 mmol), t-BuOK (6.2 g, 55 mmol), dry 2,2'-bipyridine (0.12 g, 0.85 mmol) were added into a Schlenk flask. Then anhydrous toluene (70 mL) was added to the system and stirred at 120 $^{o}$C overnight under Ar. The reaction mixture was then cooled down to room temperature and extracted with $CH_2Cl_2$, remove the solvent. The crude product was purified by column chromatography (DCM/PE = 2 : 1) to obtain the product as yellow oil (2.64 g, 35%). $^1$H NMR (400 MHz, DMSO) δ 7.32 (d, J = 6.4 Hz, 2H), 7.05 (d, J = 6.7 Hz, 4H), 6.94 (d, J = 4.3 Hz, 4H), 6.68 (d, J = 6.6 Hz, 2H), 3.75 (s, 6H).

**4-methoxy-N-(4-methoxyphenyl)-N-(4-(4,4,5,5-tetramethyl-1,3,2-dioxaborolan-2-yl)phenyl)aniline (compound 2).**

Under the protection of Ar, 4-bromoaniline (1.728 g, 3 mmol), bis(pinacolato)diboron

(0.96 g, 3.75 mmol), KOAc (0.9 g, 9.36 mmol), dry 1,4-dioxane were added into a 50 mL flask. Then $Pd_2dba_3$ (14 mg) and X-Phos (30 mg) were added to the system and stirring at 80 $^oC$ overnight. After removing the solvent, the residue mixture was purified by column chromatography ($CH_2Cl_2$/hexane = 1 : 1) to obtain the white solid (product 2, 1.10 g, 74%). $^1H$ NMR (400 MHz, DMSO) δ 7.47 (d, 2H), 6.93 (d, 4H), 6.70 (d, 4H), 6.68 (d, 2H), 3.76 (s, 6H), 1.26 (s, 12H). $^{13}C$ NMR (100 MHz, $CDCl_3$) δ 156.23, 151.44, 140.43, 135.80, 127.20, 119.47, 118.65, 114.77, 83.41, 55.48, 24.89.

**Compound 3**[3, 4]

3,6-Dibromocarbazole (0.20 g, 0.6 mmol), compound **2** (0.56 g, 1.3 mmol), 2M solution of $K_2CO_3$ (8 mmol, 1.1 g) in $H_2O$, [$Pd(PPh_3)_4$] (0.05 mmol, 60 mg) , DMF (20 mL) were added into a 50 mL Ar-protected flask. The reaction solution was kept with stirring at 90 $^oC$ for 12 h. After cooling to R.T., the reaction mixture was poured into cold $Na_2SO_4$ aqueous solution, then the crude product precipitates out as solid. The crude product was purified by column chromatography ($CH_2Cl_2$/PE = 2:1) to obtain compound **3** as light green solid (0.38 g, 81%). $^1H$ NMR (400 MHz, DMSO) δ 11.28 (s, 1H), 8.44 (s, 2H), 7.60 (d, *J* = 8.1 Hz, 6H), 7.50 (d, *J* = 6.8 Hz, 2H), 7.05 (d, *J* = 5.6 Hz, 2H), 6.92 (d, *J* = 6.6 Hz, 2H), 3.75 (s, 12H). Anal. Calcd. for $C_{52}H_{43}N_3O_4$(%): C, 80.70; H, 5.60; N, 5.43. Found: C, 80.69; H, 5.61; N, 5.42.

**3,6-N**

Compound **1** (0.31 g, 0.4 mmol), 4-bromo-N,N-dimethylaniline (0.1 g, 0.5 mmol), tBuONa (0.58 g, 6 mmol), $Pd(OAc)_2$ (45 mg, 0.2 mmol) and $P(tBu)_3$ (0.1 M in toluene, 0.3 mL) were added into a 50 mL flask. Then 15 mL dry toluene was injected in to the flask and degassed using Ar. The reaction solution was kept with stirring at reflux for 48 h. After cooling to R.T., the mixture was diluted by 30 mL $CH_2Cl_2$ and washed with 50 mL deionized water for 3 times. The organic phase was dried by $Na_2SO_4$, and removed solvent using rotary evaporator. The crude product was purified by column chromatography ($CH_2Cl_2$/PE = 3:1) to obtain **3,6-N** (0.28 g, 82%). $^1H$ NMR (400 MHz, DMSO) δ 8.56 (d, 2H), 7.64 (d, 6H), 7.42 (d, 2H), 7.32 (d, 2H), 6.99 (m, 22H), 3.76 (s,

12H), 3.03 (s, 6H). Anal. Calcd. for $C_{60}H_{52}N_4O_4$ (%) C, 80.69; H, 5.87; N, 6.27. Found: C, 80.68; H, 5.86; N, 6.28. MS (MALDI-TOF) *m/z*: [M+] calcd, 892.40; found 892.39.

**3,6-S**

The product **3,6-S** was prepared following the same procedure to synthesize **3,6-N**. Compound 4-bromothioanisole (0.1 g, 0.5 mmol) was used instead of 4-bromo-N,N-dimethylaniline. The crude product was purified by column chromatography (DCM/PE = 2:1) to obtain **3,6-S**. δ $^1$H NMR (400 MHz, DMSO) δ 8.59 (d, 2H), 7.52 (d, 12H), 7.00 (d, 20H), 3.76 (s, 12H), 2.66 (s, 3H). Anal. Calcd. for $C_{60}H_{52}N_4O_4$ (%) C, 79.08; H, 5.51; N, 4.69; S, 3.58. Found: C, 79.08; H, 5.51; N, 4.68; S, 3.57. MS (MALDI-TOF) *m/z*: [M+] calcd, 895.34; found 895.35.

**Compound 4**[5,7]

2,7-Dibromocarbazole (0.16 g, 0.5 mmol), compound **2** (0.52 g, 1.2 mmol), 2M solution of $K_2CO_3$ (8 mmol, 1.1 g) in $H_2O$, [$Pd(PPh_3)_4$] (60 mg, 0.05 mmol) , DMF (20 mL) were added into a 50 mL Ar-protected flask. The reaction solution was kept with stirring at 90 $^o$C for 12 h. After cooling to R.T., the reaction mixture was poured into cold $Na_2SO_4$ aqueous solution, then the crude product precipitates out as solid. The crude product was purified by column chromatography ($CH_2Cl_2$/PE = 1:1) to obtain compound **3** as light green solid (0.31 g, 80%). $^1$H NMR (400 MHz, DMSO) δ 8.10 (s, 1H), 7.72 – 7.48 (m, 6H), 7.40 (d, *J* = 7.5 Hz, 2H), 7.17 – 7.01 (m, 8H), 6.91 (dd, *J* = 21.1, 7.5 Hz, 14H), 3.76 (s, 12H). Anal. Calcd. for $C_{52}H_{43}N_3O_4$(%): C, 80.70; H, 5.60; N, 5.43. Found: C, 80.73; H, 5.58; N, 5.46.

**2,7-O**

Compound **1** (0.31 g, 0.4 mmol), 4-Iodoanisole (0.12 g, 0.5 mmol), tBuONa (0.58 g, 6 mmol), $Pd(OAc)_2$ (45 mg, 0.2 mmol) and $P(tBu)_3$ (0.1 M in toluene, 0.3 mL) were added into a 50 mL flask. Then 15 mL dry toluene was injected in to the flask and degassed using Ar. The reaction solution was kept with stirring at reflux for 48 h. After cooling to R.T., the mixture was diluted by 30 mL $CH_2Cl_2$ and washed with 50 mL deionized

water for 3 times. The organic phase was dried by $Na_2SO_4$, and removed solvent using rotary evaporator. The crude product was purified by column chromatography (DCM/PE = 1:1) to obtain **2,7-O** (0.27g, 78%). $^1$H NMR (400 MHz, DMSO) δ 8.26 (d, 2H), 7.61 (d, 2H), 7.58 – 7.44 (m, 6H), 7.38 (d, 2H), 7.31 – 7.17 (m, 4H), 7.15 – 7.02 (m, 8H), 7.01 – 6.87 (m, 8H), 6.85 (d, 2H), 3.89 (s, 3H), 3.75 (s, 12H). Anal. Calcd. for $C_{59}H_{49}N_3O_5$ (%) C, 80.52; H, 5.61; N, 4.77. Found: C, 80.58; H, 5.60; N, 4.73. MS (MALDI-TOF) *m/z*: [M+] calcd, 879.37; found 879.36.

**2,7-N**

The product **2,7-N** was prepared following the same procedure to synthesize **2,7-O**. Compound 4-bromo-N,N-dimethylaniline (0.1 g, 0.5 mmol) was used instead of 4-iodoanisole. The crude product was purified by column chromatography (DCM/PE = 2:1) to obtain **2,7-N**. $^1$H NMR (400 MHz, $CDCl_3$) 8.14 (d, 2H), 7.50 (m, 12H), 7.20 – 6.61 (m, 20H), 3.84 (s, 12H), 3.15 (s, 6H). Anal. Calcd. for $C_{60}H_{52}N_4O_4$ (%) C, 80.69; H, 5.87; N, 6.27. Found: C, 80.68; H, 5.89; N, 6.26. MS (MALDI-TOF) *m/z*: [M+] calcd, 892.40; found 892.42.

**2,7-S**

The product **2,7-S** was prepared following the same procedure to synthesize **2,7-O**. Compound 4-bromothioanisole (0.1 g, 0.5 mmol) was used instead of 4-iodoanisole. The crude product was purified by column chromatography (DCM/PE = 2:1) to obtain **2,7-S**. $^1$H NMR (400 MHz, $CDCl_3$) δ 8.15 (s, 2H), 7.52 (d, 12H), 7.23 – 6.56 (m, 20H), 3.85 (s, 12H), 2.62 (s, 3H). Anal. Calcd. for $C_{59}H_{49}N_3O_4S$ (%) C, 79.08; H, 5.51; N, 4.69; S, 3.58. Found: C, 79.07; H, 5.52; N, 4.67; S, 3.59. MS (MALDI-TOF) *m/z*: [M+] calcd, 895.34; found 895.36.

**A simple analysis of relative costs of 3,6-N**

We take 3,6-N as a model to analysis the synthesis costs and compare with spiro-OMeTAD. The lab synthesis cost of **3,6-N** are estimated on a model originally proposed

by Osedach *et al.*[5] Recently, Pertrus and Malinauskas *et al*.[6-8] has used the model to estimate the cost of hole transporting materials. For every synthetic step the required amounts of reactants, catalysts, reagents and solvents are calculated to obtain 1 gram of **3,6-N** are reported (Table S3).

**Table S8** Materials, quantities and cost for the synthesis of **3,6-N**.

| Chemical | Weight Reagent or solvent (g/g) | Price of chemical ($/g) | Cost of chemical ($/g product) | Total cost ($/g) |
|---|---|---|---|---|
| Compound 1 [6] | 1.11 | 19.22 | 21.33 | |
| 4-bromo-N,N-dimethylaniline | 0.36 | 4.31 | 1.55 | |
| tBuONa | 2.07 | 0.09 | 0.19 | |
| $P(tBu)_3$ | 0.1 | 7.01 | 0.70 | |
| Pd(OAc)2 | 0.16 | 24.23 | 3.88 | |
| toluene | 50 | 0.006 | 0.30 | |
| $CH_2Cl_2$ | 450 | 0.004 | 1.80 | |
| Petroleum ether | 260 | 0.003 | 0.78 | |
| **3,6-N** | | | | 30.53 |

**Table S9** Survey of the estimated chemical synthesis cost for different HTMs.

| compound | **Material cost ($/g)** | **Commercial price ($/g)** |
|---|---|---|
| **3,6-N** | 30.53 | - |
| Spiro-OMeTAD | 91.67[6-8] | 170-500[9-11] |

**Table S10** The comparison of some reported carbazole-based HTMs and **3,6-N**.

| sample | Molecular structures | Device structures | PCE (%)[a] | Dopants | Ref. PCE[b] | Ref. |
|---|---|---|---|---|---|---|
| **3,6-N** | 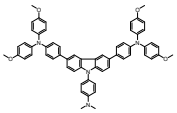 | FTO/$TiO_2$/$(FAPbI_3)_{0.85}$($MAPbBr_3)_{0.15}$/HTM | 19.25 | TBP, Li-TFSI | 19.19 | This work |
| **X25** | 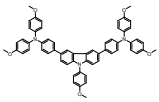 | FTO/$TiO_2$/$FA_{0.85}MA_{0.15}Pb(I_{0.85}Br_{0.15})_3$/HTM | 17.40 | TBP, Li-TFSI, FK209 | - | 9 |
| **V886** | 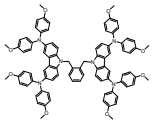 | FTO/$TiO_2$/$MAPbI_3$/HTM | 16.91 | TBP, Li-TFSI, FK209 | 18.36 | 10 |
| **V885** | 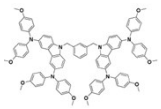 | FTO/$TiO_2$/$Cs_{0.1}(MA_{0.15}FA_{0.85})_{0.9}Pb(I_{0.85}Br_{0.15})$/HTM | 18.78 | TBP, Li-TFSI, FK209 | 18.41 | 11 |
| **LD29** | 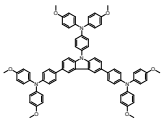 | FTO/$TiO_2$/$(FAPbI_3)_{0.85}$($MAPbBr_3)_{0.15}$/HTM | 18.09 | TBP, Li-TFSI | 18.25 | 4 |
| **pPh-2MODPACz** | 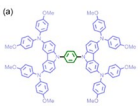 | FTO/$TiO_2$/$MAPbI_3$/HTM | 19.74 | TBP, Li-TFSI | 18.60 | 12 |
| **X50** | 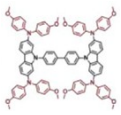 | FTO/$TiO_2$/ $(FAPbI_3)_{0.85}(MAPbBr_3)_{0.15}$/HTM | 19.20 | TBP, Li-TFSI | - | 13 |
| **X19** | 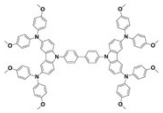 | FTO/$TiO_2$/$MAPbI_{3-x}Cl_x$/HTM | 9.8 | TBP, Li-TFSI | 10.2 | 14 |
| **BF003** | 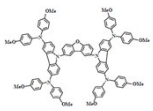 | FTO/$TiO_2$/$MAPbI_3$/HTM | 14.07 | TBP, Li-TFSI, FK209 | 15.04 | 15 |
| **3,6-Pyr** | 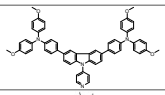 | FTO/$TiO_2$/$(FAPbI_3)_{0.85}$($MAPbBr_3)_{0.15}$/HTM | 18.45 | TBP, Li-TFSI | 17.81 | 16 |
| **SGT-405(3,6)** | 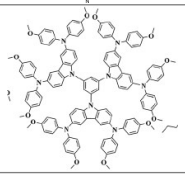 | FTO/$TiO_2$/$MAPbI_{3-x}Cl_x$/HTM | 18.87 | TBP, Li-TFSI, FK209 | 17.71 | 17 |
| **dly-2** | 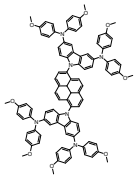 | FTO/$TiO_2$/$(FAPbI_3)_{0.75}$($MAPbI_3)_{0.17}(MAPbBr_3)_{0.08}$/HTM (planar) | 18.23 | TBP, Li-TFSI | 19.59 | 18 |

| | | | | | | |
|---|---|---|---|---|---|---|
| **JY6** | 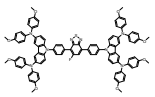 | FTO/$TiO_2$/$MAPbI_{3-x}Cl_x$/HTM (planar) | 18.54 | O2 | 16.21 | [19] |
| **BTT-3** | 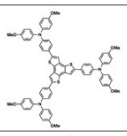 | FTO/$TiO_2$/$MAPbI_3$/HTM | 18.2 | TBP, Li-TFSI, FK209 | 18.1 | [20] |
| **BTSe-1** | 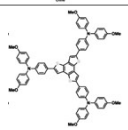 | FTO/$TiO_2$/$(FAPbI_3)_{0.85}$($MAPbBr_3)_{0.15}$/HTM | 18.5 | | 18.0 | [21] |

[a] The best PCE of developed HTMs; [b] The best PCE of standard doped Spiro-OMeTAD;

**Table S11** The comparison of some reported doped-free HTMs and **3,6-N**.

| sample | Molecular structures | Device structure | PCE (%)[a] | Ref. |
|---|---|---|---|---|
| **3,6-N** | 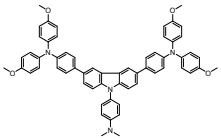 | FTO/$TiO_2$/$(FAPbI_3)_{0.85}$($MAPbBr_3)_{0.15}$/HTM | 16.21 | This work |
| **LD29** | 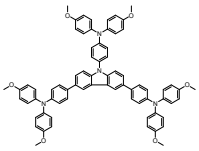 | FTO/$TiO_2$/$(FAPbI_3)_{0.85}$($MAPbBr_3)_{0.15}$/HTM | 14.29 | [4] |
| **YKP03** | 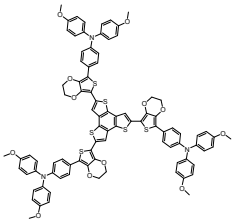 | FTO/$TiO_2$/$MAPbI_3$/HTM | 16.15 | [22] |
| **Th-TPA-4A** | 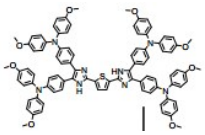 | FTO/$TiO_2$/$MAPbI_3$/HTM | 17.5 | [23] |
| **SGT-405(3,6)** | 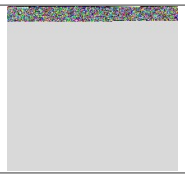 | FTO/$TiO_2$/$MAPbI_{3-x}Cl_x$/HTM | 8.48 | [17] |
| **pPh-2MODPACz** |  | FTO/$TiO_2$/$MAPbI_3$/HTM | 16.09 | [12] |

| | | | | |
|---|---|---|---|---|
| **C202** | 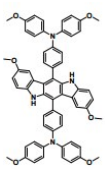 | FTO/$TiO_2$/$(FAPbI_3)_{0.85}$(MAPbBr$_3$)$_{0.15}$/HTM | 17.7 | [24] |
| **AZO-II** | 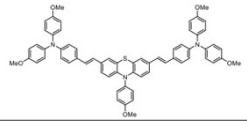 | ITO/$SnO_2$/$Cs_{0.05}MA_{1-y}FA_yPbI_{3-x}Cl_x$/HTM | 2.50 | [25] |
| **Spiro-CPDT** | 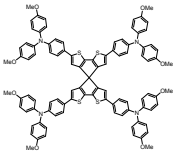 | FTO/$TiO_2$/$MAPbI_3$/HTM | 13.4 | [26] |
| **TAE-1** | 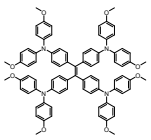 | FTO/$TiO_2$/$MAPbI_3$/HTM | 11.02 | [27] |
| **SAF-OMe** | 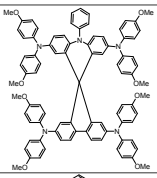 | ITO/$TiO_2$/$MAPbI_{3-x}Cl_x$/HTM | 12.39 | [28] |
| **Z1011** | 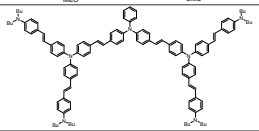 | FTO/$TiO_2$/$MAPbI_3$/HTM | 16.3 | [29] |
| **Trux 1** | 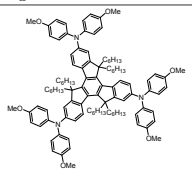 | ITO/HTM/$MAPbI_3$/PCBM/ZnO/Al | 10.2 | [30] |
| **1** | 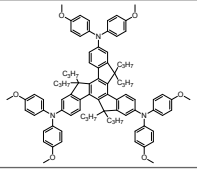 | FTO/$TiO_2$/$MAPbI_3$/HTM | 3.18 | [31] |
| **Trux-OMeTAD** | 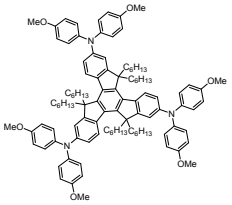 | ITO/HTM/$MAPbI_3$/PCBM/ZnO/Al | 18.6 | [32] |
| **BDT-C1** | 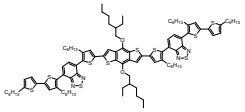 | FTO/$TiO_2$/$MAPbI_3$/HTM | 13.9 | [33] |
| **Z1013** | 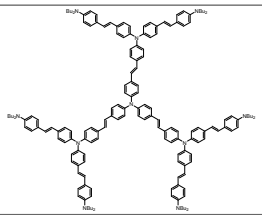 | FTO/$TiO_2$/$MAPbI_3$/HTM | 15.4 | [34] |

| | | | | |
|---|---|---|---|---|
| **2TPA-2-DP** | 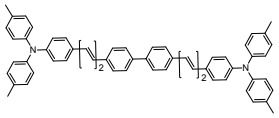 | FTO/$TiO_2$/$MAPbI_3$/HTM | 12.96 | [35] |
| **DERDTS-TBDT** | 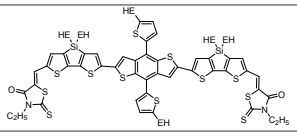 | ITO/$TiO_2$/$MAPbI_{3-x}Cl_x$/HTM/$MoO_3$ | 16.2 | [36] |
| **TPBC** | 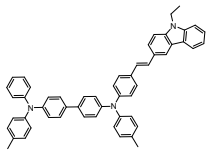 | FTO/$TiO_2$/$MAPbI_3$/HTM | 13.1 | [37] |
| **DOR3T-TBDT** | 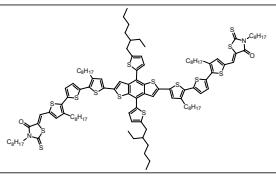 | ITO/$TiO_2$/$MAPbI_{3-x}Cl_x$/HTM/$MoO_3$ | 14.9 | [38] |
| **POZ2** | 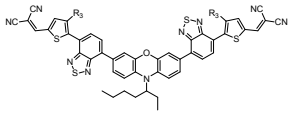 | FTO/$TiO_2$/$MAPbI_3$/HTM | 12.8 | [39] |
| **oligothiophene 1** | 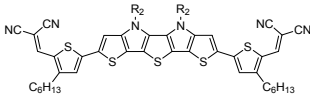 | FTO/$TiO_2$/$MAPbI_3$/HTM | 10.5 | [40] |
| **M1** | 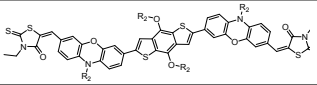 | ITO/ZnO/$PC_{70}BM$/ $MAPbI_3$/HTM | 13.2 | [41] |
| **apv-EC** | 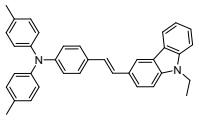 | FTO/$TiO_2$/$MAPbI_3$/HTM | 12.0 | [42] |
| **TPBC** | 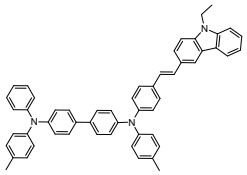 | FTO/$TiO_2$/$MAPbI_3$/HTM | 13.3 | [43] |
| **H101** | 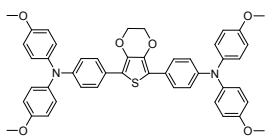 | FTO/$TiO_2$/$MAPbI_3$/HTM | 11.03 | [44] |

## References


1. C. Teng, X. Yang, C. Yang, S. Li, M. Cheng, A. Hagfeldt and L. Sun, *J. Mater. Chem. C*, 2010, **114**, 9101-9110.
2. X. Liu, F. Kong, R. Ghadari, S. Jin, W. Chen, T. Yu, T. Hayat, A. Alsaedi, F. Guo, Z. A. Tan, J. Chen and S. Dai, *Energy Technol.*, 2017, **5**, 1788-1794.
3. J. Zhang, B. Xu, M. B. Johansson, N. Vlachopoulos, G. Boschloo, L. Sun, E. M. J. Johansson and A. Hagfeldt, *ACS Nano*, 2016, **10**, 6816.

4. X. Liu, X. Ding, Y. Ren, Y. Yang, Y. Ding, X. Liu, A. Alsaedi, T. Hayat, J. Yao and S. Dai, *J. Mater. Chem. C*, 2018, **6**, 12912-12918.
5. T. P. Osedach, T. L. Andrew and V. Bulović, *Energy Environ. Sci.*, 2013, **6**, 711-718.
6. M. Petrus, T. Bein, T. Dingemans and P. Docampo, *J. Mater. Chem. A*, 2015, **3**, 12159-12162.
7. T. Malinauskas, M. Saliba, T. Matsui, M. Daskeviciene, S. Urnikaite, P. Gratia, R. Send, H. Wonneberger, I. Bruder and M. Graetzel, *Energy Environ. Sci.*, 2016, **9**, 1681-1686.
8. M. Saliba, S. Orlandi, T. Matsui, S. Aghazada, M. Cavazzini, J. P. Correabaena, P. Gao, R. Scopelliti, E. Mosconi, K. H. Dahmen, F. D. Angelis, A. Abate, A. Hagfeldt, G. Pozzi, M. Grätzel and M. K. Nazeeruddin, *Nat. Energy*, 2016, **1**, 15017.
9. J. Zhang, B. Xu, M. B. Johansson, N. Vlachopoulos, G. Boschloo, L. Sun, E. M. Johansson and A. Hagfeldt, *ACS Nano*, 2016, **10**, 6816-6825.
10. P. Gratia, A. Magomedov, T. Malinauskas, M. Daskeviciene, A. Abate, S. Ahmad, M. Grätzel, V. Getautis and M. K. Nazeeruddin, *Angew. Chem. Inter. Edit.*, 2015, **54**, 11409-11413.
11. A. Magomedov, S. Paek, P. Gratia, E. Kasparavicius, M. Daskeviciene, E. Kamarauskas, A. Gruodis, V. Jankauskas, K. Kantminiene and K. T. Cho, *Adv. Funct. Mater.*, 2018, **28**, 1704351.
12. W. Yu, Q. Yang, J. Zhang, D. Tu, X. Wang, X. Liu, G. Li, X. Guo and C. Li, *ACS Appl. Mater. Interfaces*, 2019, **11**, 30065-30071.
13. L. Wang, E. Sheibani, Y. Guo, W. Zhang, Y. Li, P. Liu, B. Xu, L. Kloo and L. Sun, *Solar RRL*, 2019.
14. B. Xu, E. Sheibani, P. Liu, J. Zhang, H. Tian, N. Vlachopoulos, G. Boschloo, L. Kloo, A. Hagfeldt and L. Sun, *Adv. Mater.*, 2014, **26**, 6629-6634.
15. Y. Shi, K. Hou, Y. Wang, K. Wang, H. Ren, M. Pang, F. Chen and S. Zhang, *J. Mater. Chem. A*, 2016, **4**, 5415-5422.
16. X. Liu, S. Ma, Y. Ding, J. Gao, X. Liu, J. Yao and S. Dai, *Solar RRL*, 2019, **3**, 1800337.
17. C. Lu, I. T. Choi, J. Kim and H. K. Kim, *J. Mater. Chem. A*, 2017, **5**, 20263-20276.
18. D. Li, J.-Y. Shao, Y. Li, Y. Li, L.-Y. Deng, Y.-W. Zhong and Q. Meng, *Chem. Commun.*, 2018, **54**, 1651-1654.
19. F. Wu, Y. Ji, C. Zhong, Y. Liu, L. Tan and L. Zhu, *Chem. Commun.*, 2017, **53**, 8719-8722.
20. A. Molina‐Ontoria, I. Zimmermann, I. Garcia‐Benito, P. Gratia, C. Roldán‐Carmona, S. Aghazada, M. Graetzel, M. K. Nazeeruddin and N. Martín, *Angew. Chem. Inter. Edit.*, 2016, **55**, 6270-6274.
21. I. García‐Benito, I. Zimmermann, J. Urieta‐Mora, J. Aragó, J. Calbo, J. Perles, A. Serrano, A. Molina‐Ontoria, E. Ortí and N. Martín, *Adv. Funct. Mater.*, 2018, **28**, 1801734.
22. Y.-K. Peng, K.-M. Lee, C.-C. Ting, M.-W. Hsu and C.-Y. Liu, *J. Mater. Chem. A*, 2019, **7**, 24765-24770.
23. J.-Y. Feng, K.-W. Lai, Y.-S. Shiue, A. Singh, P. K. CH, C. T. Li, W.-T. Wu, J. T. Lin, C. W. Chu and C.-C. Chang, *J. Mater. Chem. A*, 2019.
24. B. Cai, X. Yang, X. Jiang, Z. Yu, A. Hagfeldt and L. Sun, *J. Mater. Chem. A*, 2019, **7**, 14835-14841.
25. J. Salunke, X. Guo, Z. Lin, J. R. Vale, N. R. Candeias, M. Nyman, S. Dahlström, R. Österbacka, A. Priimagi and J. Chang, *ACS Appl. Energy Mater.*, 2019, **2**, 3021-3027.
26. M. Franckevičius, A. Mishra, F. Kreuzer, J. Luo, S. M. Zakeeruddin and M. Grätzel, *Mater, Horiz.*, 2015, **2**, 613-618.
27. L. Cabau, I. Garcia-Benito, A. Molina-Ontoria, N. F. Montcada, N. Martin, A. Vidal-Ferran and E. Palomares, *Chem. Commun.*, 2015, **51**, 13980-13982.
28. Y. K. Wang, Z. C. Yuan, G. Z. Shi, Y. X. Li, Q. Li, F. Hui, B. Q. Sun, Z. Q. Jiang and L. S. Liao, *Adv.*

*Funct. Mater.*, 2016, **26**, 1375-1381.

29. F. Zhang, C. Yi, P. Wei, X. Bi, J. Luo, G. Jacopin, S. Wang, X. Li, Y. Xiao and S. M. Zakeeruddin, *Adv. Energy Mater.*, 2016, **6**, 1600401.
30. R. Grisorio, R. Iacobellis, A. Listorti, L. De Marco, M. P. Cipolla, M. Manca, A. Rizzo, A. Abate, G. Gigli and G. P. Suranna, *ACS Appl. Mater. Interfaces*, 2017, **9**, 24778-24787.
31. J. Wang, Y. Chen, M. Liang, G. Ge, R. Zhou, Z. Sun and S. Xue, *Dyes Pigments*, 2016, **125**, 399-406.
32. C. Huang, W. Fu, C.-Z. Li, Z. Zhang, W. Qiu, M. Shi, P. Heremans, A. K.-Y. Jen and H. Chen, *J. Am. Chem. Soc.*, 2016, **138**, 2528-2531.
33. C. Chen, M. Cheng, P. Liu, J. Gao, L. Kloo and L. Sun, *Nano Energy*, 2016, **23**, 40-49.
34. F. Zhang, X. Zhao, C. Yi, D. Bi, X. Bi, P. Wei, X. Liu, S. Wang, X. Li and S. M. Zakeeruddin, *Dyes and Pigments*, 2017, **136**, 273-277.
35. L. Zhu, J. Xiao, J. Shi, J. Wang, S. Lv, Y. Xu, Y. Luo, Y. Xiao, S. Wang and Q. Meng, *Nano Research*, 2015, **8**, 1116-1127.
36. Y. Liu, Z. Hong, Q. Chen, H. Chen, W. H. Chang, Y. Yang, T. B. Song and Y. Yang, *Adv. Mater.*, 2016, **28**, 440-446.
37. Y. Song, S. Lv, X. Liu, X. Li, S. Wang, H. Wei, D. Li, Y. Xiao and Q. Meng, *Chem. Commun.*, 2014, **50**, 15239-15242.
38. Y. Liu, Q. Chen, H.-S. Duan, H. Zhou, Y. M. Yang, H. Chen, S. Luo, T.-B. Song, L. Dou and Z. Hong, *J. Mater. Chem. A*, 2015, **3**, 11940-11947.
39. M. Cheng, B. Xu, C. Chen, X. Yang, F. Zhang, Q. Tan, Y. Hua, L. Kloo and L. Sun, *Adv. Energy Mater.*, 2015, **5**, 1401720.
40. P. Qin, H. Kast, M. K. Nazeeruddin, S. M. Zakeeruddin, A. Mishra, P. Bäuerle and M. Grätzel, *Energy & Environmental Science*, 2014, **7**, 2981-2985.
41. M. Cheng, C. Chen, X. Yang, J. Huang, F. Zhang, B. Xu and L. Sun, *Chem. Mater.*, 2015, **27**, 1808-1814.
42. S. Lv, Y. Song, J. Xiao, L. Zhu, J. Shi, H. Wei, Y. Xu, J. Dong, X. Xu and S. Wang, *Electrochimica Acta*, 2015, **182**, 733-741.
43. S. Lv, L. Han, J. Xiao, L. Zhu, J. Shi, H. Wei, Y. Xu, J. Dong, X. Xu and D. Li, *Chem. Commun.*, 2014, **50**, 6931-6934.
44. H. Li, K. Fu, A. Hagfeldt, M. Grätzel, S. G. Mhaisalkar and A. C. Grimsdale, *Angew. Chem. Inter. Edit.*, 2014, **126**, 4169-4172.